Atmospheric turbulence effect on ranging of the interferometric direction device

G.A. Kaloshin and I.P. Lukin

Institute of Atmospheric Optics,
Siberian Branch of the Russian Academy of Sciences, Tomsk

Theoretical assessments of the dependence of interferometric direction device range on laser beam parameters, device geometry, and atmospheric turbulence characteristics are presented in this work. The assessments are calculated for three values of interference contrast (0.1, 0.3, and 0.5), structure parameter of turbulent atmosphere permittivity fluctuations within the $10^{-16} \ldots 10^{-13}$ m$^{-2/3}$ range, distances between the radiating apertures centers, equal to 1, 2, 3, 4, and 5 cm, and three radiation wavelengths (0.51, 0.63, and 1.06 μm). It is shown that the range of interferometric direction device exceeds 5 km at average turbulence intensities corresponding to most realizable in the marine and coastal atmosphere in midlatitudes and low interference contrast, equal to 0.1.

Introduction

The state-of-the-art development of photoacoustic devices allows their wide application to laser beam control in space.[1] Modern photoacoustic grating deflectors (PAD) have a high resolution and a fast response. They allow both random continuous scan of a laser beam and discrete turn to any allowed direction. All this, along with simple design, easy control, low power consumption, and small size, attract interest to the PAD use for laser aids of navigation (LAN). A key moment in this case is a possibility of high-precision direction specification, which is very important, since the motion direction specification is the main problem of LAN along with designation of navigation hazards.

A method has been worked out,[2–4] when synchronous scanning of two laser beams, the wave interference is produced in the region of their superposition; and the frequency of the resultant oscillation uniquely correlates with the direction to the source.

It is known that the possibility of the interference contrast registration is determined by the random inhomogeneities of the air permittivity on the path.

Therefore, it is of interest to estimate the method range depending on the turbulence characteristics and parameters of the device optical scheme.

1. Interferometric specification of the direction

The optical schematic of a device, realizing this method for one-dimensional case, is shown in Fig. 1. (For two-dimensional case, the laser beam is scanned over two coordinates using either two one-dimensional PADs in tandem or one PAD cell, in which two orthogonal acoustic waves are excited).

A laser beam consequently passes through two acoustic cells PAD-1 and PAD-2, in which medium density changes under ultrasound influence with the help of a wobbler. Acoustic waves produce a phase grating, where laser radiation is diffracted. Using the shore device collimators, diffracted beams are brought out to the orientation zone next a beacon, where they produce an interference pattern in the mixture region. An on-board photodetector registers and separates the received signal frequency, uniquely correlating with the direction to the beacon.
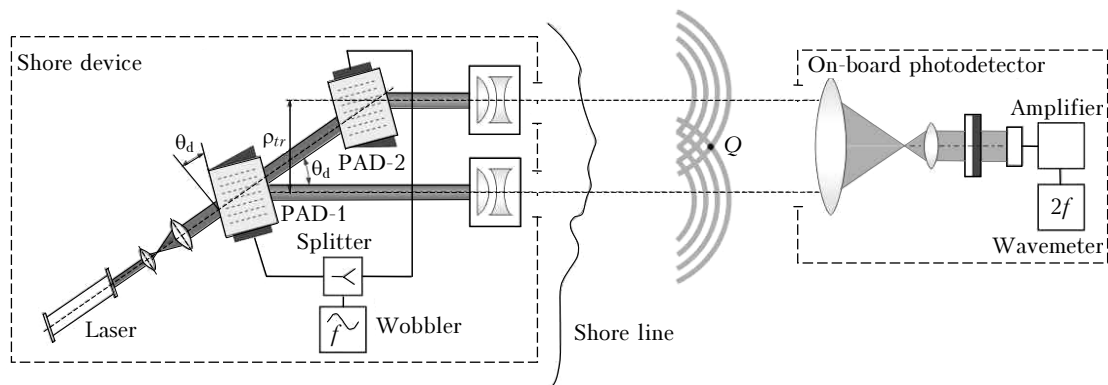
Fig. 1. Optical schematic of the laser interferometric direction device.

The position of laser beams in space is determined by the relation $\sin\theta_d = \lambda f_a / v_a$, where θ_d is the diffraction (scanning) angle; λ is the optical radiation wavelength in vacuum; f_a is the acoustic wave frequency; v_a is the acoustic wave speed in PAD. At small diffraction angles, we can write $\theta_d \cong \lambda f_a / v_a$; $\theta_d \cong 2°$ for a He–Ne laser ($\lambda = 0.63 \ \mu m$) and acoustic wave frequency $f_a = 10 \cdot 10^6$ Hz. If θ_d is 10-fold increased by means of optical amplification, the frequency, corresponding to 1 ang. s, is equal to 5.5 kHz. Hence, direction specification to within 1 ang. s is not a technical problem.

2. Distortions of a PAD-formed interference pattern

2.1. Problem statement

Different facets of interference pattern formation in turbulent atmosphere have been studied in Refs. 5–10. The most close variant of interferometer schematic was considered in Ref. 7, where fluctuations of the interference pattern, formed in turbulent atmosphere by two mutually coherent spaced point sources of optical radiation (interference of two spherical waves), were analyzed. For our purposes, we generalize the results of Ref. 7 to a more realistic model of optical radiation source.

Accept the following scheme of the beacon and photodetector: coherent radiation sources, located at the points $\{0, \rho_1\}$ and $\{0, \rho_2\}$ respectively, emit laser beams parallel to each other and OX-axis in direction of positive x; the photodetector is located at the point Q (see Fig. 1) with the coordinates $\{x, \rho\}$. Consider $\rho_{tr} = (\rho_2 - \rho_1)$ as a vector of spacing of radiation sources, forming the interference pattern.

Let optical radiation of each source be a partially coherent Gaussian beam with the initial amplitude E_0, initial radius a_0, radius of wave front curvature in the center of radiating aperture R_0, and initial coherence radius ρ_k. The assumption about full identity of sources slightly simplifies the problem, but does not restrict it seriously. The photodetector is a quadratic detector, reacting to the arriving radiation power, signal of which can be written in the form

$$i_r(x, \rho) = \eta_0 I(x, \rho),$$

where η_0 is the coefficient of photodetector effective quantum efficiency; $I(x, \rho)$ is the instantaneous interference pattern intensity at the detector point, which can be written as

$$I(x, \rho) = U_1(x, \rho) U_1^*(x, \rho) + U_2(x, \rho) U_2^*(x, \rho) +$$
$$+ 2\text{Re}\{U_1(x, \rho) U_2^*(x, \rho)\}; \qquad (1)$$

$U_j(x, \rho)$ is the optical wave field of one source; $j = 1, 2$. For definiteness, $\rho_1 = -\rho_{tr}/2$ and $\rho_2 = \rho_{tr}/2$ (OX-axis in this case passes through the middle of the interference pattern).

2.2. Mean intensity of a PAD-formed interference pattern

The equation describing the function of mutual second-order coherence of the fields of two Gaussian optical radiation beams[6] for the above-formulated boundary conditions when using quadratic approximation of the complex optical wave phase has the following solution:

$$\langle U_j(x, \rho) U_{j'}^*(x, \rho) \rangle =$$

$$= \frac{U_0^2 a_0^2}{a^2(x)} \exp\left[-\frac{(\rho - \rho_j)^2}{2a^2(x)} - \frac{(\rho - \rho_{j'})^2}{2a^2(x)} - i\frac{\delta(x)}{a^2(x)}(\rho_j - \rho_{j'})\rho + \right.$$
$$\left. + i\frac{\delta(x)}{2a^2(x)}\left(\rho_j^2 - \rho_{j'}^2\right) - \frac{(\rho_j - \rho_{j'})^2}{\rho_c^2(x)} \right], \qquad (2)$$

where

$$a(x) = a_0 \sqrt{(1-\mu)^2 + \Omega_0^{-2}\left(1 + \frac{a_0^2}{\rho_k^2} + \frac{4}{3}\frac{a_0^2}{\rho_0^2}\right)}$$

is the current mean radius of optical radiation beam;

$$\delta(x) = \Omega_0\left[-\mu(1-\mu) + \Omega_0^{-2}\right]$$

is the geometrical factor; $\delta(x)/[ka^2(x)]$ is the current mutual curvature of mean wave fronts of optical radiation beams;

$$\rho_c(x) = \sqrt{3}\,\rho_0 \sqrt{\frac{(1-\mu)^2 + \Omega_0^{-2}\left(1 + \frac{a_0^2}{\rho_k^2} + \frac{4}{3}\frac{a_0^2}{\rho_0^2}\right)}{\left(\mu^2 + \Omega_0^{-2}\right)\left(1 + \frac{3}{4}\frac{\rho_0^2}{\rho_k^2}\right)}}$$

is the current radius of mutual coherence of two optical beams; $\mu = x/R_0$ is the focusing parameter; $\Omega_0 = ka_0^2 / x$ is the Fresnel number of radiating aperture; $k = 2\pi/\lambda$ is the optical wave number;

$$\rho_0 = \left(2^{-5/3}\frac{18}{5}0.033\,\pi^2\frac{\Gamma(7/6)}{\Gamma(11/6)}C_\varepsilon^2 k^2 x\right)^{-3/5}$$

is the radius of plane optical wave coherence in turbulent atmosphere; C_ε^2 is the structure parameter of turbulent atmosphere permittivity fluctuations; j, $j' = 1, 2$.

Using Eqs. (1) and (2), obtain the equation for mean intensity of the interference pattern, formed by two partially coherent laser beams:

$$\langle I(x, \rho) \rangle = 2\frac{U_0^2 a_0^2}{a^2(x)} \exp\left[-\frac{\rho^2 + \rho_{tr}^2/4}{a^2(x)} \right] \times$$

$$\times \left\{ \cosh\left[\frac{\rho_{tr}\rho}{a^2(x)}\right] + \exp\left[-\frac{\rho_{tr}^2}{\rho_c^2(x)}\right]\cos\left[\frac{\delta(x)}{a^2(x)}\rho_{tr}\rho\right] \right\}. \ (3)$$

When scanning two laser beams simultaneously with PAD-1 and PAD-2 with the angle $\pm\theta_d$ relative

to the direction, specified by the *OX*-axis, the interference pattern at the point *Q* is displaced to $\pm x\theta_d$ from the direction.

2.3. Formulation of conditions for choice of parameters of the beacon optical scheme

Simple and obvious conditions restricting the choice of parameters of laser beams and beacon scheme are formulated on the base of Eq. (3) at standard parameters of the turbulent atmosphere over the sea surface.[11,12]

Linear dimensions $l_{int}(x)$ of the region, where interference pattern (3) has been formed, approximately equals to the laser beam diameter if $a(x) \gg \rho_{tr}$:

$$l_{int}(x) \cong 2a(x). \qquad (4)$$

The interference band maxima are located at the points ρ_{max}, defined[3] by the equation

$$\frac{\delta(x)}{a^2(x)}\rho_{tr}\rho_{max} = 2n\pi, \ n = 0, \pm 1, \pm 2, \ldots,$$

while the minima — at the points ρ_{min}:

$$\frac{\delta(x)}{a^2(x)}\rho_{tr}\rho_{min} = (2n+1)\pi, \ n = 0, \pm 1, \pm 2, \ldots.$$

For simplicity, assume $\rho \parallel \rho_{tr}$, then

$$\rho_{max} \parallel \rho_{min} \parallel \rho_{tr} \ \text{and} \ \rho_{max} = \frac{2n\pi a^2(x)}{\delta(x)\rho_{tr}},$$

$$\rho_{min} = \frac{(2n+1)\pi a^2(x)}{\delta(x)\rho_{tr}}.$$

In this case, the interference band width $\Delta l_{int}(x)$ can be assessed by the equation

$$\Delta l_{int}(x) = 2|\rho_{max} - \rho_{min}| = \frac{2\pi a^2(x)}{\delta(x)\rho_{tr}}. \qquad (5)$$

At the same time, the visibility of distortions of mean-intensity interference pattern is

$$v(x) = \frac{\langle I(x,\rho_{max})\rangle - \langle I(x,\rho_{min})\rangle}{\langle I(x,\rho_{max})\rangle + \langle I(x,\rho_{min})\rangle} =$$

$$= \left\{ e^{-\frac{\rho_{max}^2}{a^2(x)}} \cosh\left[\frac{\rho_{tr}\rho_{max}}{a^2(x)}\right] - e^{-\frac{\rho_{min}^2}{a^2(x)}} \cosh\left[\frac{\rho_{tr}\rho_{min}}{a^2(x)}\right] + \right.$$

$$\left. + \left[e^{-\frac{\rho_{max}^2}{a^2(x)}} + e^{-\frac{\rho_{min}^2}{a^2(x)}} \right] \exp\left[-\frac{\rho_{tr}^2}{\rho_c^2(x)}\right] \right\} \Bigg/$$

$$\Bigg/ \left\{ e^{-\frac{\rho_{max}^2}{a^2(x)}} \cosh\left[\frac{\rho_{tr}\rho_{max}}{a^2(x)}\right] + e^{-\frac{\rho_{min}^2}{a^2(x)}} \cosh\left[\frac{\rho_{tr}\rho_{min}}{a^2(x)}\right] + \right.$$

$$\left. + \left[e^{-\frac{\rho_{max}^2}{a^2(x)}} - e^{-\frac{\rho_{min}^2}{a^2(x)}} \right] \exp\left[-\frac{\rho_{tr}^2}{\rho_c^2(x)}\right] \right\}.$$

It is allowable to consider $\rho_{max} \approx \rho_{min} \approx \rho$, then

$$v(x) \cong \frac{1}{\cosh\left[\frac{\rho_{tr}\rho}{a^2(x)}\right]} \exp\left[-\frac{\rho_{tr}^2}{\rho_c^2(x)}\right]. \qquad (6)$$

It is evident that the method works only if at least one complete interference band is in the field of interference pattern; therefore, the below condition follows from Eqs. (4) and (5):

$$l_{int}(x) \ge \Delta l_{int}(x).$$

This equation is fulfilled providing the distance between coherent radiation sources meets the condition:

$$\rho_{tr} \ge \pi\frac{a(x)}{\delta(x)}. \qquad (7)$$

In addition, the visibility of the middle interference pattern (when $\cosh[\rho_{tr}\rho/a^2(x)] \cong 1$) is satisfactory as long as the coherence radius of registered optical field at the observation point exceeds the magnitude of transversal beams shift, i.e.:

$$\rho_{tr} \le \sqrt{-\ln[v(x)]}\,\rho_c(x), \qquad (8)$$

obtained by simplifying Eq. (6).

Thus, summing Eqs. (7) and (8), obtain the following equation:

$$\pi\frac{a(x)}{\delta(x)} \le \rho_{tr} \le \sqrt{-\ln[v(x)]}\,\rho_c(x). \qquad (9)$$

To fulfill Eq. (9), the right part at least has to exceed the left one:

$$\pi\frac{a(x)}{\delta(x)} \le \sqrt{-\ln[v(x)]}\,\rho_c(x),$$

or, in the other form:

$$\frac{\pi a_0}{\sqrt{-\ln[v(x)]}}\frac{\sqrt{\left(\mu^2 + \Omega_0^{-2}\right)\left(\dfrac{1}{3\rho_0^2} + \dfrac{1}{4\rho_k^2}\right)}}{\Omega_0\left[-\mu(1-\mu) + \Omega_0^{-2}\right]} \le 1.$$

The last is equivalent (in case of collimated beams $\mu = 0$) to the requirement for the initial laser beam sizes a_0 to obey the condition

$$a_0 \le \frac{\sqrt{-\ln[v(x)]}}{\pi}\frac{1}{\sqrt{\dfrac{1}{3\rho_0^2} + \dfrac{1}{4\rho_k^2}}}. \qquad (10)$$

It is evident that $a_0 \le \left\{\sqrt{3}\sqrt{-\ln[v(x)]}/\pi\right\}\rho_0$ at large values of initial laser beam coherence $\rho_k \to \infty$, i.e., initial radii of Gaussian optical beams are mainly determined by the loss of the optical radiation coherence along the propagation path due to atmosphere turbulence, while at $\rho_k \to 0$ $a_0 \le \left\{2\sqrt{-\ln[v(x)]}/\pi\right\}\rho_k$ is

determined by the initial coherence of the source. Note that Eq. (10) imposes quite hard restrictions on the laser beam parameters for horizontal atmospheric paths not longer than 10 km; only sufficiently narrow and high-coherent laser beams can satisfy these restrictions.

3. Choice of parameters of the beacon optical scheme

3.1. Restrictions to the initial laser beam apertures

Figure 2 shows the behavior of the function

$$f_1(x) = \frac{\sqrt{-\ln[v(x)]}}{\pi} \frac{1}{\sqrt{\dfrac{1}{3\rho_0^2} + \dfrac{1}{4\rho_k^2}}},$$

equal to the right part of Eq. (10), at different values of the parameters. Curves 1, 2, and 3 present the influence of λ on $f_1(x)$: $1 - \lambda = 0.51$, $2 - 0.63$, and $3 - 1.06\,\mu m$ (other parameters are the following: $\rho_k = 2$ cm, $v(x) = 0.1$, $C_\varepsilon^2 = 10^{-13}$ m$^{-2/3}$); curves 3, 4, and 5 show the $f_1(x)$ sensitivity to the interference contrast $v(x)$: $3 - v(x) = 0.1$, $4 - 0.3$, $5 - 0.5$ (in this case, $\lambda = 1.06\,\mu m$, $\rho_k = 2$ cm, $C_\varepsilon^2 = 10^{-13}$ m$^{-2/3}$), and curves 3, 6, 7, and 8 show the $f_1(x)$ dependence on the level of turbulent atmosphere permittivity fluctuations C_ε^2: $3 - C_\varepsilon^2 = 10^{-13}$ m$^{-2/3}$, $6 - 10^{-14}$, $7 - 10^{-15}$, $8 - 10^{-16}$ m$^{-2/3}$ ($\lambda = 1.06\,\mu m$, $\rho_k = 2$ cm, $v(x) = 0.1$). Since the initial laser beam size is to obey the condition $a_0 \leq f_1(x)$, the initial values of laser beam radii can be chosen on the base of the data in Fig. 2. It turns out that Eq. (10) is fulfilled within a path length range 1–10 m provided the initial laser beam radius a_0 does not exceed 1...2 mm.
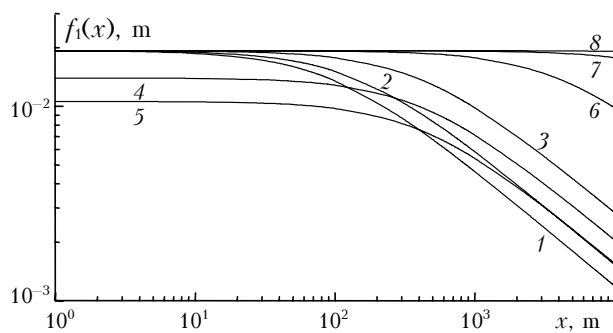
Fig. 2. Plots of $f_1(x)$ for the choice of initial values of laser beam parameters.

For further assessments, the following values of Gaussian laser beam parameters are used: $a_0 = 1...2$ mm, $R_0 \to \infty$, $\rho_k = 1...2$ cm, $\lambda = 0.51$; 0.63; $1.06\,\mu m$. For such laser beams, the angular beam width $\psi_0 \cong \dfrac{2}{ka_0}\sqrt{1 + a_0^2/\rho_k^2}$ should not exceed $\approx 1'$ in the region, where the directional pattern has been formed.

3.2. Restrictions to the distance between laser beams

Equation (9) at known parameters of optical beams allows one to choose the distance ρ_{tr} between radiation sources, forming the interference pattern. Figure 3 shows the functions

$$f_2(x) = \pi \frac{ka_0^3}{x}\sqrt{1 + \frac{x^2}{k^2 a_0^4}\left(1 + \frac{a_0^2}{\rho_k^2} + \frac{4}{3}\frac{a_0^2}{\rho_0^2}\right)}$$

(solid lines)

and

$$f_3(x) = \sqrt{-\ln[v(x)]}\sqrt{\frac{1 + \dfrac{x^2}{k^2 a_0^4}\left(1 + \dfrac{a_0^2}{\rho_k^2} + \dfrac{4}{3}\dfrac{a_0^2}{\rho_0^2}\right)}{\dfrac{1}{3\rho_0^2} + \dfrac{1}{4\rho_k^2}}}\frac{ka_0^2}{x}$$

(dashed lines),

calculated for different values of the parameters. Curves 1, 2, and 3 present the influence of λ on $f_2(x)$ and $f_3(x)$: $1 - \lambda = 0.51$, $2 - 0.63$, and $3 - 1.06\,\mu m$ (in this case, $a_0 = 2$ mm, $\rho_k = 2$ cm, $v(x) = 0.1$, $C_\varepsilon^2 = 10^{-16}$ m$^{-2/3}$), curves 3, 4, and 5 are calculated respectively for the following values of interference contrast $v(x)$: $0.1\,(3)$, $0.3\,(4)$, and $0.5\,(5)$ (the following parameters are the same: $\lambda = 1.06\,\mu m$, $a_0 = 2$ mm, $\rho_k = 2$ cm, $C_\varepsilon^2 = 10^{-16}$ m$^{-2/3}$), and curves 3, 6, 7, and 8 — for different levels of turbulent atmosphere permittivity fluctuations C_ε^2: $C_\varepsilon^2 = 10^{-16}$ m$^{-2/3}$ (3), 10^{-15} (6), 10^{-14} (7), and 10^{-13} m$^{-2/3}$ (8) ($\lambda = 1.06\,\mu m$, $a_0 = 2$ mm, $\rho_k = 2$ cm, $v(x) = 0.1$). Since the spacing ρ_{tr} of radiation sources, forming the interference pattern, should be more than $f_2(x)$ and less than $f_3(x)$, the acceptable ρ_{tr} values are estimated from Fig. 3 within the 1–5 cm range for path lengths from 20 m to 10 km. These values of radiation sources spacing are used in further assessments.
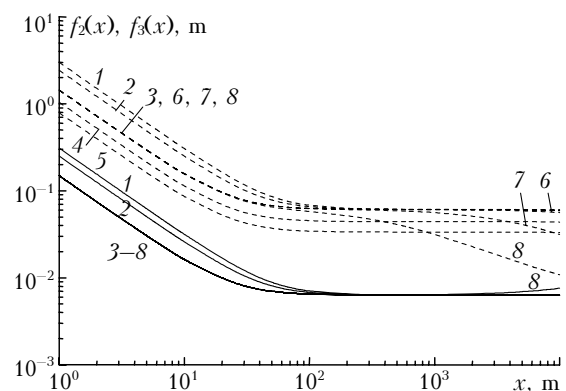
Fig. 3. Functions $f_2(x)$ (solid lines) and $f_3(x)$ (dashed lines) for the choice of the spacing value for laser beam optical axes.

4. Assessment of the laser beacon ranging

The assessment consists in solving the nonlinear equation

$$x = f_4(x), \qquad (11)$$

where

$$f_4(x) = \frac{\sqrt{-\ln\left[v(x)\right]}}{\rho_{tr}} \sqrt{\frac{1 + \dfrac{x^2}{k^2 a_0^4}\left(1 + \dfrac{a_0^2}{\rho_k^2} + \dfrac{4}{3}\dfrac{a_0^2}{\rho_0^2}\right)}{\left(\dfrac{1}{3\rho_0^2} + \dfrac{1}{4\rho_k^2}\right)}} \, k a_0^2.$$

Equation (11) was solved by the simple iteration method.

The assessment results for laser beacon ranging (see Fig. 1) are shown in Figs. 4–6 for all values of structure parameter of air permittivity fluctuations, realizable in the surface layer,[11,12] for three values of interference pattern visibility and optical radiation wavelengths.
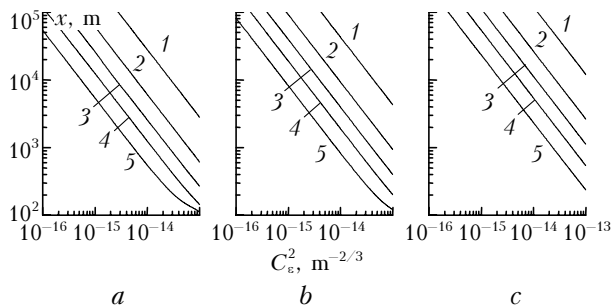
Fig. 4. Laser beam range as a function of atmospheric turbulence structure parameter at interference pattern visibility $v(x) = 0.1$ at radiation wavelength $\lambda = 0.51$ (a), 0.63 (b), and 1.06 μm (c) and the distance between beam centers $\rho_{tr} = 0.01$ (1), 0.02 (2), 0.03 (3), 0.04 (4), and 0.05 m (5).
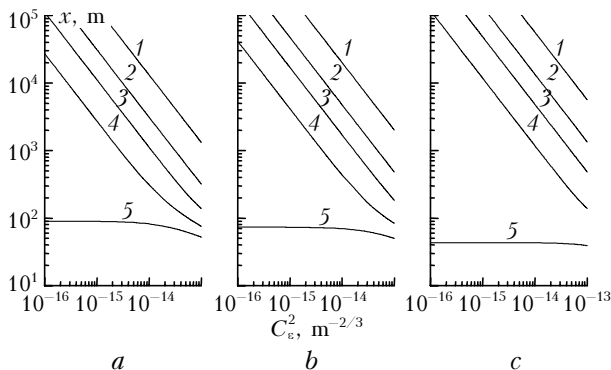
Fig. 5. The same as in Fig. 4 for the interference pattern visibility $v(x) = 0.3$.

It was considered that laser radiation propagated along horizontal path at a height of 10…20 m above the water surface.

Conclusions

The main conclusions which can be drawn from the results, presented in this work, are the following.

1. The closer the optical radiation sources, the lower the contrast value of the registered interference pattern; the larger the radiation wavelength, the larger the laser beacon ranging.
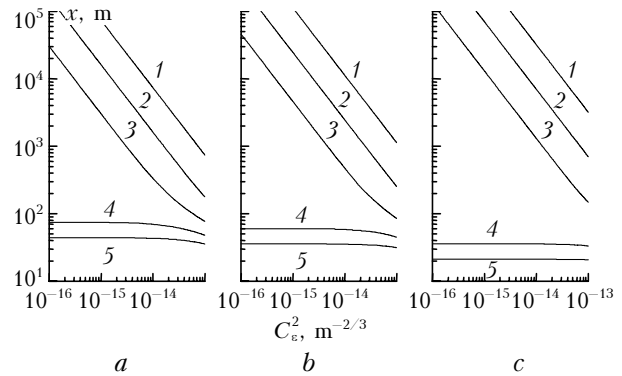
Fig. 6. The same as in Fig. 4 for the interference pattern visibility $v(x) = 0.5$.

2. The device ranging, depending on geometry of optical elements, exceeds 5 km at low interference pattern contrast $v(x) = 0.1$, $\lambda = 0.51$ μm, source spacing from 1 to 5 cm, and mean turbulence intensity $10^{-15}\,\text{m}^{-2/3}$, mostly realizable in the marine and coastal atmosphere in mid-latitudes.

3. At higher contrast values of the interference pattern, the laser beacon operates in a smaller spacing range ρ_{tr} of radiation sources, forming the interference pattern (from 1 to 4 cm for $v(x) = 0.3$ and from 1 to 3 cm at $v(x) = 0.5$).

Thus, the technique for the choice of interference laser beacon parameters, proving for a required range of beacon operation above the sea surface at any possible values of turbulence parameters of weakly turbid atmosphere, is described based on the analysis of mean intensity of the PAD-formed interference pattern.

References

1. V.N. Balakshii, V.N. Parygin, and L.E. Chirkov, *Physical Grounds for Photoacoustics* (Radio i Svyaz', Moscow, 1985), 280 pp.
2. G.A. Kaloshin and V.M. Shandarov, *"The device for moving objects orientation,"* Inventor's Cerificate No. 1554605 SSSR, MKI4 G01s17/00, G01c21/04.
3. G.A. Kaloshin and V.M. Shandarov, *"The method for moving objects orientation,"* Inventor's Cerificate No. 1804214 SSSR, MKI4 G01s17/00.
4. G.A. Kaloshin, I.P. Lukin, and V.M. Shandarov, in: *Proc. of the IVth Russian Sci. and Tech. Conf. "State-of-the-art and Problems of Navigation and Oceanology"* (State Research Institute for Navigation and Hydrography, St. Petersburg, 2001), V. 2, pp. 26–29.
5. M. Born and E. Wolf, *Principles of Optics* (Pergamon, New York, 1959).
6. V.E. Zuev, V.A. Banakh, and V.V. Pokasov, *Optics of Turbulent Atmosphere* (Gidrometeoizdat, Leningrad, 1988), 271 pp.
7. I.P. Lukin and V.L. Mironov, Radiotekhn. Elektron. **22**, No. 3, 615–618 (1977).
8. I.P. Lukin, Opt. Spekstrosk. **44**, Is. 6, 1153–1156 (1978).
9. I.P. Lukin, Opt. Spekstrosk. **52**, Is. 1, 108–111 (1982).
10. I.P. Lukin, Atmos. Oceanic Opt. **6**, No. 12, 884–887 (1993).
11. P.K. Pasricha and B.M. Reddy, Proc. IEE **137**, Pt. F., No. 5, 384–386 (1990).
12. J.L. Forand and D. Dion, Proc. SPIE **2828**, 129–140 (1996).